Available online at www.sciencedirect.com

SciVerse ScienceDirect

Ceramics International 39 (2013) 8507–8512

CERAMICS INTERNATIONAL

www.elsevier.com/locate/ceramint

Short communication

The effect of particle size in freeze casting of porous alumina–zirconia composite

Gang Liu*, Tim W. Button

School of Metallurgy and Materials, University of Birmingham, Edgbaston, Birmingham, B15 2TT, UK

Received 10 September 2012; received in revised form 26 February 2013; accepted 26 February 2013
Available online 14 March 2013

Abstract

The freeze casting technique was employed to fabricate porous alumina–zirconia composite ceramics. The composite ceramics showed lamellar morphologies. The porosity decreased from 74% to 35%, whilst the initial solids loading increased from 11 vol% to 30 vol%. The chemical composition analysis by EDX indicated that the phase segregation occurred due to different particle sizes and densities. Engulfment could be induced by variation of particle size. Moreover, the particle size can also affect the mechanical properties of the ceramics.

Keywords: Freeze casting; Ceramic; Size effect

1. Introduction

Porous ceramics have been extensively used in a wide range of applications [1–5], including ceramic filters, catalysts supports, bone scaffolds, porous piezoelectric materials, and as electrodes in fuel cells. Among many fabrication techniques for porous ceramics, the freeze casting [6–9] technique has attracted considerable attention in the past several years as a cost effective and environmentally-friendly process. Water and camphene are the two most frequently used solvents in freeze casting. In the case of water as the solvent, the final porous ceramics normally exhibit lamellar microstructures [10]. When camphene is used as the solvent, the final porous ceramics normally exhibit three-dimensional interconnected microstructures [11]. To date, many factors affecting the porosity and mechanical properties of the final porous ceramic, such as initial solids loading, cooling rate, sintering temperature, and additive content, have been widely investigated [4,6,10–13], and many significant improvements have been achieved. Nevertheless, the effect of particle size of the ceramic powder constituent in freeze casting has attracted little attention. In the present study, a water-based ceramic slurry system containing two ceramic phases with different particle sizes was chosen and their influence in freeze casting has been investigated and explained.

2. Experimental procedure

As received yttira-stabilized zirconia fine power (d_{50}~0.1 μm, Tosoh-zirconia, Japan), yttira-stabilized zirconia coarse powder (d_{50}~0.7 μm, FYT13-002H, Unitec, Stafford, U.K.), and alumina powder (d_{50}~0.7 μm, CT300SG, Caldic) were utilized as the ceramic phases in the slurries. Distilled water was employed as the vehicle. Ammonium polyacrylate (NH_4PAA) 0.65 wt% (based on the dry ceramic powder) solution (D3021, Duramax, Chesham Chemicals Ltd., UK) was utilized as the dispersant (with a concentration of 0.14 wt%). 3 wt% B-1000 and 2 wt% B-1007 binders (acrylic polymer emulsion, Duramax, UK) were added into the slurries as a binder.

All the aqueous ceramic slurries were prepared by mixing distilled water, dispersant and ceramic powders under constant stirring, followed by ball-milling for 24 h with zirconia (or alumina) media. Binders were added to the slurries before casting. The resultant ceramic slurries were poured into a transparent silicone mold (12 mm diameter × 13.5 mm height), which was then transferred to a stainless steel cold finger placed in a container filled with liquid nitrogen. The solidification rates in the axial direction of the cylindrical

*Corresponding author. Tel.: +44 121 414 43442; fax: +44 121 414 7468.
E-mail addresses: liugangxjtu@gmail.com, liugu@bham.ac.uk (G. Liu).

0272-8842/$ - see front matter © 2013 Elsevier Ltd and Techna Group S.r.l. All rights reserved.
http://dx.doi.org/10.1016/j.ceramint.2013.02.101

sample used in this study were 110 μms^{-1} and 45 μms^{-1}. The frozen samples were demoulded and transferred into a freeze dryer (Labconco Corp., Kansas City, MO, USA) for 24 h for sublimation. The sintering was carried out in air under a constant heating rate of 1 °C/min to 500 °C to burn out the binder, followed by 5 °C/min to 1550 °C for 2 h. After sintering, samples were cut along the direction perpendicular to the solidification direction using a precision diamond saw (Struers Accutom-50, Denmark) for microstructural observation. The rheological properties of the slurries were measured through a rheometer (Carri-med 115/A) with a cone and plane system (Truncation: 59 μm; Core: 4 cm, 20°) at room temperature. The porosity was measured by mercury porosimetry (Autopore III 9400, Micromeritics, US). The compressive strength was measured using an Instron testing machine (Model 4467, United Kingdom) with a crosshead speed of 0.2 mm/min. The shrinkage of the samples was obtained using measurements of sample dimensions before and after sintering. The microstructures of the samples were analyzed by scanning electron microscopy (SEM) (JSM 7000, Jeol, Tokyo, Japan). Energy dispersive X-ray (EDX) was done using an Oxford Inca EDX system to evaluate the chemical composition of the samples. Six EDX measurements were taken for each point and the average values are presented in Table 1.

Table 1
Chemical composition of the sintered composite ceramic walls and arms (the initial mole ratio is 60.3/100).

	Location	Al/Zr (mole)
Fig. 3(a)	(1) Ceramic wall	56.5/100
	(2) Ceramic arm	319.1/100
Fig. 3(b)	(1) Ceramic wall	57.8/100
	(2) Ceramic arm	637.5/100

3. Results and discussion

Fig. 1 shows SEM micrographs of a cross-section of the sintered Al_2O_3–ZrO_2 composite ceramics obtained from slurries with the same Al/Zr mole ratio of 60.3:100 but with different solids loadings. All porous Al_2O_3–ZrO_2 ceramics exhibited relatively homogeneous lamellar microstructures with long-range channels, with the thickness of the lamellae increasing with a corresponding increase in the solids loading. The ceramic walls were relatively dense and showed a special morphology; one side was smooth whereas the other exhibited ceramic arms. The total porosity of these samples decreased from about 74% to 35% as the initial solids loading was increased from 11 vol% to 30 vol%, as shown in Fig. 2. The relationship between the porosity and the initial solids loading can be expressed as follows:

$$P = 98.6 - 2.1S \quad (1)$$

where P is the porosity, and S is the initial solids loading.

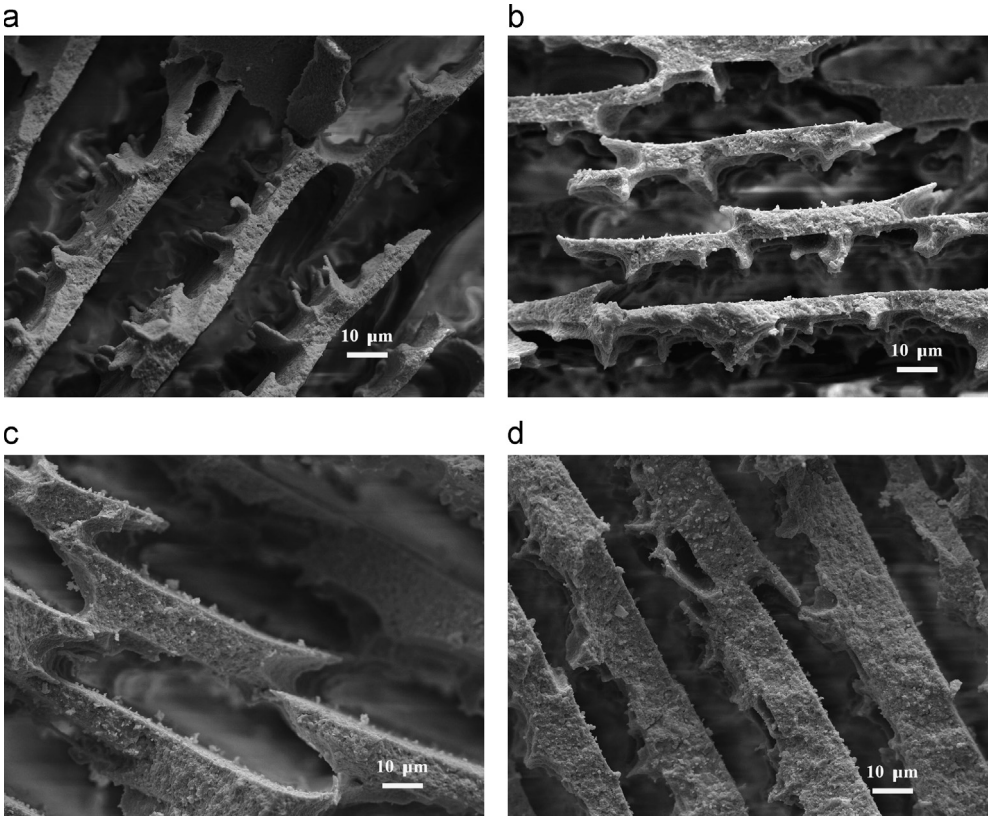

Fig. 1. Cross-sectional micrographs of the sintered Al_2O_3–ZrO_2 composite ceramics obtained from slurries with differing initial solids loading: (a) 11 vol%, (b) 16 vol%, (c) 22 vol%, (d) 30 vol% and under a solidification rate of 110 μms^{-1}. Solidification direction is perpendicular to the page and the zirconia powder used here is the fine powder.

Lower initial solids loading leads to higher porosity, which is in agreement with the trend reported in the literature [10,12,13].

One interesting phenomenon was observed in the porous Al_2O_3–ZrO_2 composite ceramics. The chemical compositions of the lamellae and arms were measured by EDX, as indicated in Fig. 3(a) and (b), and presented in Table 1. The results revealed a similar tendency in all samples irrespective of the initial solids loading. Compared to the initial Al/Zr mole ratio (60.3:100), the element ratio at the location of the ceramic wall was slightly lower but the element ratio at the location of the ceramic arms was much higher, indicating a "phase segregation" occurring during the freeze casting process in these samples.

It is not easy to make an accurately quantitative explanation due to the lack of experimental and published literature data about the interface. As we know, the most important forces for a spherical particle close to the solidification front, are the repulsive force F_R and attractive drag force F_η, which are expressed as [14]

$$F_R = 2\pi r \Delta\sigma_0 \left(\frac{a_0}{d}\right)^n \tag{2}$$

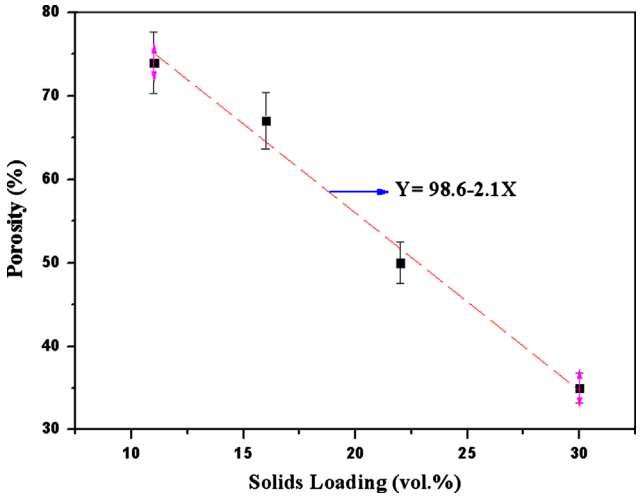

Fig. 2. The porosity of the porous Al_2O_3–ZrO_2 composite ceramics as a function of initial solids loading (Fine zirconia powder was used here and the solidification rate was 110 μms^{-1}).

$$F_\eta = \frac{6\pi\eta v r^2}{d} \tag{3}$$

where $\Delta\sigma_0$ is the interface free energy, a_0 is the average intermolecular distance in the film, d is the overall thickness, η is the slurry viscosity, r is the particle radius, n is an exponent and ν is the velocity.

Moreover, the Newton's second law of motion is expressed as

$$F = ma \tag{4}$$

where F is the force applied on the object, m is the mass of the object, and a is the accelerated speed. And the mass m for a spherical particle can be express as

$$m = \frac{4}{3}\pi r^3 \rho \tag{5}$$

where ρ is the density of the particle.

At the beginning of freezing, the dominant force for a particle is the repulsive force F_R (the attractive drag force F_η can be ignored.). According to Eqs. (2), (4) and (5), the accelerated speed for a particle in the interface can be expressed as

$$a = \frac{3}{2}\frac{\Delta\sigma_0}{r^2\rho}\left(\frac{a_0}{d}\right)^n \tag{6}$$

During freezing, alumina and zirconia ceramic particles were ejected by the moving ice front. As shown in the experimental, the alumina and zirconia particles have different particle sizes (0.7 μm for alumina, and 0.1 μm for fine zirconia particles) and densities (3.99 g/cm^3 for alumina and 6.10 g/cm^3 for zirconia). According to Eq. (6), the zirconia particles obtain a larger accelerated speed than the alumina particles, and therefore move further away from the ice crystals before the equilibrium in the interface is achieved. Hence, the zirconia particles are mostly concentrated at the location of the ceramic walls which are further away from the ice crystals, and form a Zr-rich zone, whilst the alumina particles mostly settled down in the vicinity of the ceramic arms (closer to the ice crystals) and formed an Al-rich zone. It can be concluded that in freeze casting, especially in a two-phase system, the particle size and the density of the ceramic powders becomes very critical.

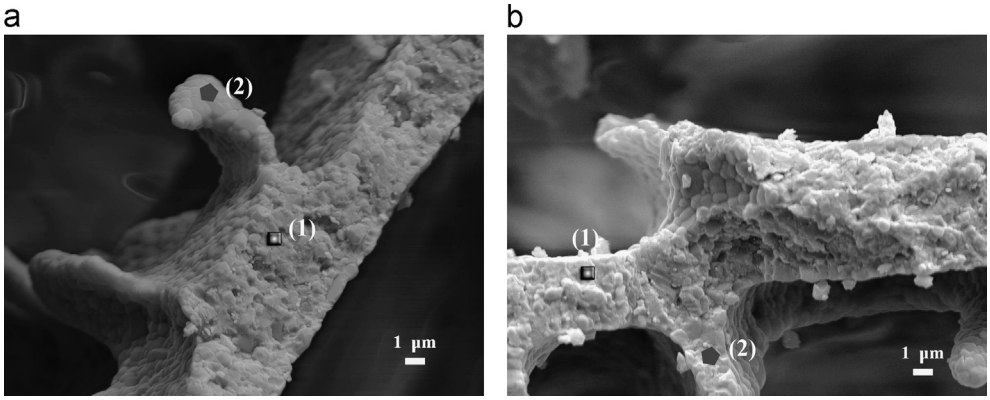

Fig. 3. SEM photos of ceramic walls and arms for chemical compositional analysis by EDX: (a) 11 vol% initial solids loading, and (b) 16 vol% initial solids loading (Fine zirconia powder was used here and the solidification rate was 110 μms^{-1}).

Another interesting phenomenon was observed when the ratio of Al_2O_3 and ZrO_2 was changed. Fig. 4(a)–(d) shows the cross-sectional micrographs of porous ceramics obtained from the 42 vol% slurries but with either different Al/Zr mole ratios or particle sizes. The sample shown in Fig. 4(a) was pure alumina (Al/Zr 100:0, by mole) porous ceramic. It can be seen that engulfment occurred and the lamellae architecture lost. The sample shown in Fig. 4(b) is the Al_2O_3–ZrO_2 composite ceramic with an Al/Zr, ratio of 1:1 (by mole). Engulfment also occurred in this sample, though the tracks of lamellae structures can still be observed. The sample shown in Fig. 4(c) and (d) were 100% zirconia (0:100, Al/Zr by mole) porous ceramics but obtained from different powders. Engulfment occurred in the sample obtained from coarse powders as shown in Fig. 4(c),

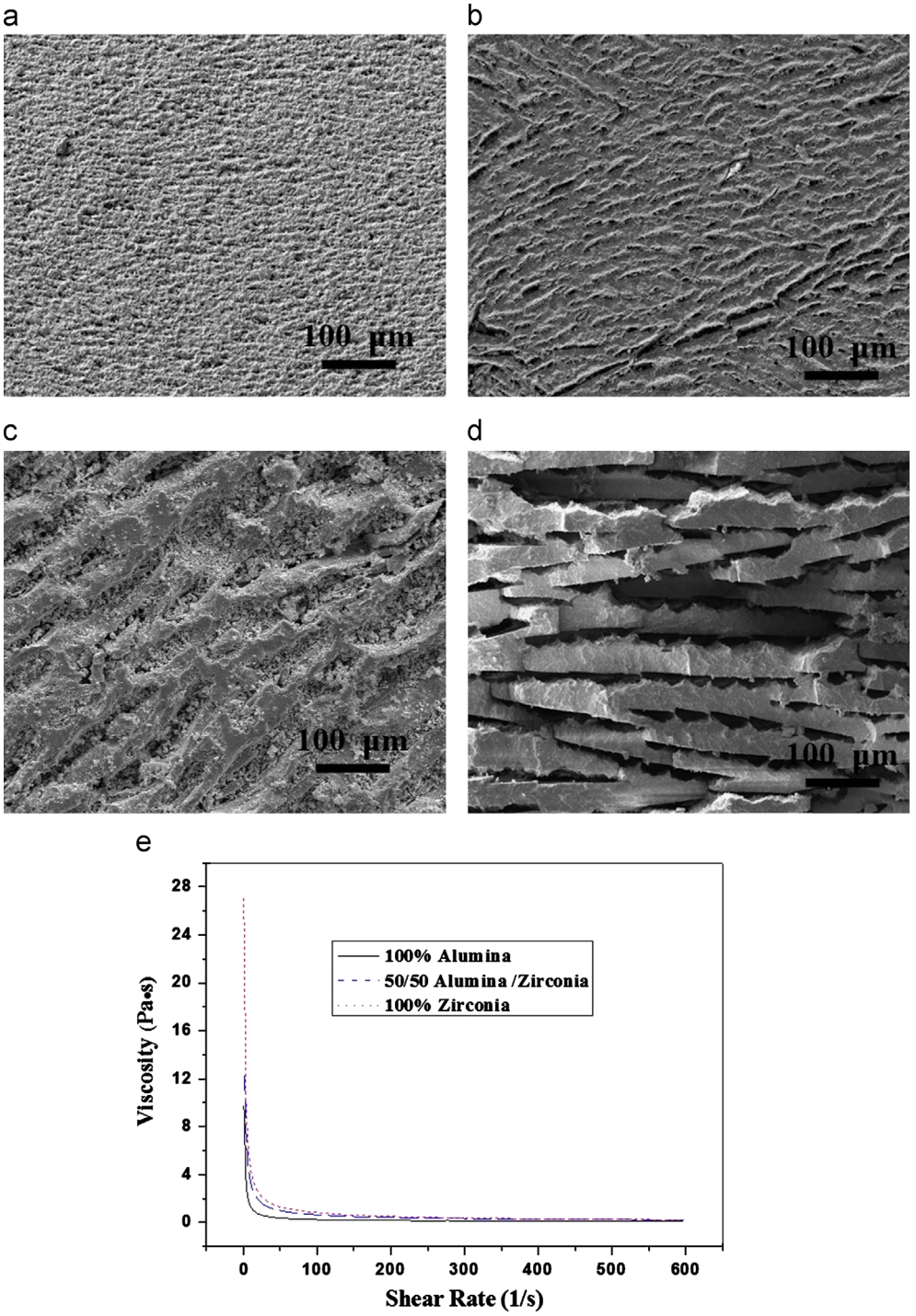

Fig. 4. Cross-sectional micrographs of porous ceramic or composite ceramics obtained from 42 vol% initial solids loading, same solidification rate (110 μms^{-1}), but with different Al/Zr mole ratios or particle sizes: (a) 100/0 (b) 100/100 (fine powder) (c) 0/100 (coarse powder), (d) 0/100 (fine powder) and (e) viscosity of the suspensions versus shear rates.

though the tracks of lamellae structures could also be observed. However, engulfment did not occur in the sample obtained from fine powders as shown in Fig. 4(d) and the lamellae structures still existed.

According to Eqs. (2) and (3), a critical velocity ν_c for a certain particle size exists in the process of freeze casting, above which the particle cannot be ejected by the moving solidification front and engulfment occurs. The critical velocity is shown below [14,15]:

$$\upsilon_c = \frac{\Delta\sigma d}{3\eta R}\left(\frac{a_0}{d}\right)^n \tag{7}$$

Four samples were obtained under the same solidification rate and from slurries with the same solids loading of 42 vol%. The difference is either the alumina content or the particle size. The slurries used to prepare the three samples (Fig. 4(a), (b) and (d)) all exhibited shear-thinning rheological behavior as shown Fig. 4(e). The initial viscosity (when the shear rate is close to zero) in Fig. 4(e) is the closest value to the viscosity of the slurry when the freezing starts (27 pa s for 100% zirconia (fine powder), 12 pa s for 50/50 alumina/zirconia, and 9.5 pa s 100% alumina). As mentioned previously, the alumina powder has a particle size around 0.7 μm, while that of the fine zirconia powder is 0.1 μm. According to the simple model shown in Eq. (7), the ν_c is mainly determined by viscosity and particle size. The viscosity ratio of 100% zirconia and 100% alumina is less than 3, while the particle size ratio of zirconia and alumina is about 1:7. Therefore, the alumina particles have relatively smaller critical velocity according to Eq. (7). Correspondingly, it is much likely that under the same solidification rate, the samples containing alumina particles may easily reach their critical velocities, resulting in the engulfment observed in these samples; however, the 100% zirconia sample shown in Fig. 4(d) did not reach its critical velocity. Moreover, the comparison between the pure ZrO_2 samples in Fig. 4(c) and (d) indicates that engulfment is highly likely to occur in slurry with larger particle sizes when the processing conditions are very similar. Hence, the particle size and slurry viscosity have a significant impact on the critical velocity in a two-phase slurry system.

Furthermore, the compressive strengths of the porous zirconia (single phase) ceramics and zirconia–alumina composites were measured and several physical properties are shown in Table 2. The shrinkages of these samples after sintering in two directions (either parallel or perpendicular to the ice growth direction) were measured. When the zirconia particle size increased from 0.1 μm to 0.7 μm, the shrinkage of the ceramic with single phase decreased in both directions. The smaller particle size is very helpful to improve the densification of zirconia ceramics. As we know, larger shrinkage leads to lower porosity. Hence, the porosity increased from 70% to 76% as shown in Table 2. The composite ceramics showed a very similar tendency, in that the shrinkage also decreased when the particle size increased. Correspondingly, their porosities increased from 74% to 79% when the particle size increased. Normally, the compressive strength is generally related to the porosity according to Rice's equation using an exponential relationship as [16]:

$$E = E_0 e^{-bP} \tag{8}$$

where E_0 is the zero-porosity compressive strength, b reflects the particle stacking and shape, and P is the volume fraction porosity.

It is not difficult to conclude that larger porosity leads to lower mechanical properties derived from Eq. (8). Therefore, when the particles size increased, the compressive strength of the zirconia ceramics decreased from 4.3 MPa to 1.7 MPa and that of zirconia–alumina composites decreased from 6.8 MPa to 1.9 MPa, as shown in Table 2.

Table 2
Physical properties of porous ceramics or composites.

Composition	Porosity (%)	Compressive strength (MPa)	Shrinkage rate along S_{d1}[a] (%)	Shrinkage rate along S_{d2}[a] (%)
Fine ZrO_2	70	4.3±0.8	22.5	25.5
Coarse ZrO_2	76	1.7±0.2	13.3	21.8
Composite (fine ZrO_2 with Al_2O_3)	74	6.8±0.7	21.5	26.1
Composite (coarse ZrO_2 with Al_2O_3)	79	1.9±0.6	10.2	19.6

[a] S_{d1} is parallel to the ice front direction; S_{d2} is perpendicular to the ice front. All of the samples here were obtained from 20 vol% slurries under a solidification rate of 45 μms^{-1}. For the composites, the Al/Zr (by mole) is 1:1.

4. Conclusions

In summary, the porosity of the porous Al_2O_3–ZrO_2 (fine powder) composites decreased from 74% to 35% when the solids loading increased from 11 vol% to 30 vol% under solidification rates of 110 μms^{-1}. The particle size and the density of alumina and zirconia powders are very critical in this two-phase slurry system. The zirconia particles (0.1 μm) can obtain a larger accelerated speed, mostly concentrated at the location of the ceramic walls, and thus form Zr-rich zones; while the alumina particles (0.7 μm) mostly settled down in the vicinity of the ceramic arms, and formed Al-rich zones. Meanwhile, the particle size and viscosity of slurries have significant effect on the critical velocity during freezing. Furthermore, the particle size also has an important effect on the final mechanical properties because the powders with smaller particle size improve the densification of ceramics or composites and lead to lower porosity.

References

[1] A.R. Studart, U.T. Gonzenbach, E. Tervoort, L.J. Gauckler, Processing routes to macroporous ceramics: a review, Journal of the American Ceramic Society 89 (2006) 1771–1789.
[2] P. Sepulveda, J.G.P. Binner, Processing of cellular ceramics by foaming and in situ polymerisation of organic monomers, Journal of the European Ceramic Society 19 (1999) 2059–2066.
[3] P. Colombo, Conventional and novel processing methods for cellular ceramics, Philosophical Transactions of the Royal Society A-Mathematical Physical and Engineering Sciences 364 (2006) 109–124.
[4] S. Deville, E. Saiz, A.P. Tomsia, Freeze casting of hydroxyapatite scaffolds for bone tissue engineering, Biomaterials 27 (2006) 5480–5489.

[5] Y.-H. Koh, I.-K. Jun, J.-J. Sun, H.-E. Kim, In situ fabrication of a dense/porous Bi-layered ceramic composite using freeze casting of a ceramic–camphene slurry, Journal of the American Ceramic Society 89 (2006) 763–766.
[6] S.W. Sofie, F. Dogan, Freeze casting of aqueous alumina slurries with glycerol, Journal of the American Ceramic Society 84 (2001) 1459–1464.
[7] S. Deville, E. Saiz, R.K. Nalla, A.P. Tomsia, Freezing as a path to build complex composites, Science 311 (2006) 515–518;
S. Deville, R.K. Nalla, Freezing as a path to build complex composites, Science 312 (2006) 1321.
[8] H.F. Zhang, I. Hussain, M. Brust, M.F. Butler, S.P. Rannard, A.I. Cooper, Aligned two- and three-dimensional structures by directional freezing of polymers and nanoparticles, Nature Materials 4 (2005) 787–793.
[9] S. Deville, Freeze-casting of porous ceramics: a review of current achievements and issues, Advanced Engineering Materials 10 (2008) 155–169.
[10] S. Deville, E. Saiz, A.P. Tomsia, Ice-templated porous alumina structures, Acta Materialia 55 (2007) 1965–1974.
[11] K. Araki, J.W. Halloran, Porous ceramic bodies with interconnected pore channels by a novel freeze casting technique, Journal of the American Ceramic Society 88 (2005) 1108–1114.
[12] Y.H. Koh, J.H. Song, E.J. Lee, H.E. Kim, Freezing dilute ceramic/camphene slurry for ultra-high porosity ceramics with completely interconnected pore networks, Journal of the American Ceramic Society 89 (2006) 3089–3093.
[13] B.H. Yoon, Y.H. Koh, C.S. Park, H.E. Kim, Generation of large pore channels for bone tissue engineering using camphene-based freeze casting, Journal of the American Ceramic Society 90 (2007) 1744–1752.
[14] C. Korber, G. Rau, M.D. Cosman, E.G. Cravalho, Interaction of particles and a moving ice–liquid interface, Journal of Crystal Growth 72 (1985) 649–662.
[15] G. Liu, D. Zhang, C. Meggs, T.W. Button, Porous Al(2)O(3)–ZrO(2) composites fabricated by an ice template method, Scripta Materialia 62 (2010) 466–468.
[16] D.M. Liu, Influence of porosity and pore size on the compressive strength of porous hydroxyapatite ceramic, Ceramics International 23 (1997) 135–139.